Linearized spectral decimation in fractals

Askar A. Iliasov [1,*] Mikhail I. Katsnelson [1] and Shengjun Yuan[2,1,†]

[1]*Institute for Molecules and Materials, Radboud University, Heyendaalseweg 135, 6525AJ Nijmegen, The Netherlands*
[2]*School of Physics and Technology, Wuhan University, Wuhan 430072, China*

In this article, we study the energy spectrum of fractals which has block-hierarchical structure. We develop a method to study the spectral properties in terms of linearization of spectral decimation procedure and verify it numerically by calculation of level-spacing distributions. Our approach provides qualitative explanation for various spectral properties of self-similar graphs within the theory of dynamical systems, including the power-law level-spacing distribution, smooth density of states, and effective chaotic regime.

I. INTRODUCTION

Fractals were intensively studied in the 1980s. Recent developments of experimental techniques [1–6] open possibilities to study condensed-matter systems with complex geometries (for example, fractals) at the atomic level. Many theoretical and numerical works on fractals appeared recently including the studies on transport and optical properties [7–11], electronic localization [12–15], topology of fractals [16–20], appearance of flatbands [21–24], and others [25–28].

One of the unique features of a fractal is its hierarchical block structure, which repeats itself from one scale to another. It is known that, for a simple fractal (such as Sierpinski gasket), the renormalization group induces a spectral decimation procedure for the spectrum or the density of states, which can be interpreted as a direct renormalization on the spectrum [29]. However, it is unclear whether there is a general approach for fractals with complex structure.

A lot of fractal-like structures admit a spectral decimation procedure. In other words, there is a connection between scale in the real space and scale in the energy spectrum, and the spectrum itself is a limit set of some iterated functions. Spectral properties, however, still depend strongly on the system. In some cases, the spectrum is a union of Cantor set with some degenerate eigenvalues [30]; in other cases, the limit spectrum can be a smooth function [31–33]. Numerical studies of quasiperiodic potentials show that their level-spacing distribution follows a power law [34,35]. For iterations of nonlinear functions, it was shown that sometimes they also have power-law level-spacing distributions [35,36].

It is not clear yet how to determine the spectral behavior of a fractal, in general. Even if a spectral decimation procedure does exist, it is not sufficient to make a certain statement about the spectrum. Of course, it seems almost impossible to build a precise theory, but it is possible to build an effective theory neglecting some details of graph geometry.

In this article, we present a linearized version of spectral decimation, which can be applied for graphs built iteratively from a simple block. We show that with linearized spectral decimation functions, one can qualitatively describe level-spacing distribution for hierarchical graphs and deduce possible phase transitions. Observed transitions can be interpreted as chaos-order transitions.

The paper is organized as follows. In Sec. II, we describe the algebraic setup for our approach. In Sec. III, we describe the linearized version of the spectral decimation procedure in terms of dynamical systems. In Sec. IV, we apply this method to some practical cases. In Sec. V, we discuss the connection to other physical properties, such as the electronic conductivity. Finally, a brief summary of our study is given in Sec. VI. The Appendix describes the geometrical interpretation of our model.

II. TENSOR STRUCTURE OF SCALES

A. Representation of fractals

A fractal can be described by one-particle tight-binding Hamiltonian,

$$H = -\sum_{\langle ij \rangle} t_{ij} c_i^\dagger c_j, \qquad (1)$$

which describes electrons with hopping between the nearest-neighbor sites $\langle ij \rangle$ of a fractal, $c_i^\dagger$ and c_j are creation and annihilation fermionic operators. We can regard this Hamiltonian as an adjacency matrix A of a graph. The adjacency matrix is a square matrix A such that its element A_{ij} is one when there is an edge from vertex i to vertex j, and zero when there is no edge (if an electron can jump from one site to another there is an edge connecting two sites).

Let us consider a fractal with hierarchical block structure. This graph structure induces a block structure in the adjacency matrix. For example, if A_k is an adjacency matrix of kth iterations of a fractal, then, the diagonal submatrices will be equal to A_{k-1}, which is an adjacency matrix of previous iteration. The nondiagonal submatrices represent connections

*A.Iliasov@science.ru.nl
†s.yuan@whu.edu.cn

between different blocks. If there is no connection between blocks on the first iteration, there will be no connection further, and corresponding nondiagonal submatrices will be always zero. So, for A_k, we can write an expression using the Kronecker product of matrices $\otimes$ (which has properties of a tensor product),

$$A_k = A_{k-1} \otimes 1 + \sum_\alpha C_{k-1,\alpha} \otimes a_\alpha, \qquad (2)$$

where matrices $C_{k,\alpha}$ describe detailed connections between blocks, a_α are built from the adjacency matrix of the first iteration of a fractal $a = A_0$. Every matrix a_α has one nonzero component in the way that $a = \sum a_\alpha$. So, matrices a_α represent nonzero connections between different blocks of a fractal.

To build matrices $C_{k,\alpha}$, we start with the second iteration,

$$A_2 = a \otimes 1 + \sum_\alpha c_\alpha \otimes a_\alpha, \qquad (3)$$

where matrices c_α define the detailed connections between different blocks of a fractal. Since fractals have self-similar structures, we can write that

$$C_{k,\alpha} = \underbrace{c_\alpha \otimes c_\alpha \cdots \otimes c_\alpha}_{k \ times} = c_\alpha^{\otimes k}. \qquad (4)$$

Then, for the kth iteration, we have

$$A_k = A_{k-1} \otimes 1 + \sum_\alpha c_\alpha^{\otimes(k-1)} \otimes a_\alpha, \qquad (5)$$

which can be also expressed as

$$A_k = a \otimes 1^{\otimes(k-1)} + \sum_{l=1}^{k-1} \sum_\alpha c_\alpha^{\otimes l} \otimes a_\alpha \otimes 1^{\otimes(k-l-1)}. \qquad (6)$$

The above expression shows how adjacency matrices of fractals are constructed from basic blocks representing a hierarchical structure without geometric details (via the first iteration of a fractal) and detailed connections between blocks. It is easy to check that fractals, such as the Sierpinski carpet and the extended Sierpinski gasket can be constructed following Eq. (6).

B. Spectral properties of tensor products

From the algebraic point of view, we can see that, in some simple cases, different scales are decoupled. For example, in the case of Cartesian products $H \square G$ of graphs H and G, its adjacency matrix is $A_{H \square G} = A_H \otimes 1 + 1 \otimes A_G$, then, the eigenvectors of this adjacency matrix are tensor products of eigenvectors of A_H and A_G. Therefore, we obtain

$$A_{H \square G}(\psi_{Hi} \otimes \psi_{Gj}) = (\lambda_{Hi} + \lambda_{Gj})\psi_{Hi} \otimes \psi_{Gj}, \qquad (7)$$

where λ_H and λ_G are eigenvalues of matrices H and G. It indicates that the spectrum of the Cartesian products of two graphs is the sum of each individual spectrum.

A straightforward way to generalize the result of Eq. (7) is to increase the number of summands and the number of tensor products as the following:

$$A_h = \sum_\alpha \Pi_\beta^\otimes h_{\alpha\beta}, \qquad (8)$$

where $h_{\alpha\beta}$ is a set of matrices. If $[h_{\alpha\beta}, h_{\alpha'\beta}] = 0$ for every fixed β, i.e., all matrices of the same scale commute. Then, eigenvectors of the matrix A_h are tensor products of eigenvectors of $h_{\alpha\beta}$. The spectrum will be sums of products of the corresponding eigenvalues.

Unfortunately, this approach cannot be applied directly to fractals because of the noncommutativity of matrices c_α and a_α in Eq. (6). But one can perform an estimation by a kind of algebraic averaging, which can be interpreted as a mean-field theory, to overcome the difficulty raised by the noncommutative matrices.

In order to do this, let us first consider a matrix with the form

$$A_k^{sum} = a \otimes 1^{\otimes(k-1)} + \sum_{l=1}^{k-1} c^{\otimes l} \otimes a \otimes 1^{\otimes(k-l-1)}, \qquad (9)$$

where $c = \sum c_\alpha$ and $a = \sum a_\alpha$. The matrix A_k^{sum} has a similar structure as A_k in Eq. (6) with a_α and c_α replaced by their sums. One can also see that A_k^{sum} can be written as a sum of various graphs A_k including all possible permutations of indices α. If we assume that different variants of organizing connections between blocks are equal, i.e., we neglect detailed geometry, then, we can write $c_\alpha = \epsilon c$, where $\epsilon^{-1} = n_c$ is the number of c_α. Having performed that, we obtain a weighted version of Eq. (9),

$$\hat{A}_k = a \otimes 1^{\otimes(k-1)} + \sum_{l=1}^{k-1} \epsilon^l c^{\otimes l} \otimes a \otimes 1^{\otimes(k-l-1)}. \qquad (10)$$

Now, the only condition remaining that needed to be satisfied was the commutativity of a and c. However, in some cases, such as an extended Sierpinski gasket, c is proportional or even equal to a, then, we can calculate the spectrum analytically as the following.

If $c = a$, the spectrum of $\hat{A}_k$ is given by the formula:

$$\sigma(\hat{A}_k) = \left\{ \lambda_{i_1} + \epsilon \lambda_{i_1} \lambda_{i_2} + \epsilon^2 \lambda_{i_1} \lambda_{i_2} \lambda_{i_3} \right.$$
$$\left. + \cdots + \epsilon^{k-1} \lambda_{i_1} \lambda_{i_2} \cdots \lambda_{i_k} \right\}, \qquad (11)$$

where λ_i are eigenvalues of the matrix a. Lower indices mean that, to obtain one specific eigenvalue in $\sigma(\hat{A}_k)$, one needs to choose the k eigenvalues of a $\{\lambda_{i_1}, \lambda_{i_2}, \ldots, \lambda_{i_k}\}$ and substitute them into the expression of Eq. (11). All possible choices give the whole spectrum of the $\hat{A}_k$.

One can note a similarity between Eq. (11) and the conventional renormalization approach in quantum field theory [37]. Because of the noncommutativity of block matrices c_α, the correct spectral decimation functions are nonlinear. We approximate a nonlinear function by a linear one as an analogy to the one-loop approximation and, then, iterate this linear function repeatedly in order to include all scales.

III. CORRESPONDING DYNAMICAL SYSTEM

In the last section, we obtained an expression for the spectrum of fractal graphs neglecting geometry details. In this section, we reformulate this expression in terms of the spectral renormalization group, which is also called spectral decimation (for some fractals, such as Sierpinski gasket, there are exact nonlinear functions producing the spectrum). This

approximation is a dynamical system obtained as a multi-valued linear function with slopes equal to eigenvalues of a simple block λ_i normalized to the number of connections between blocks.

We use dynamical systems in order to represent the spectrum of Hamiltonian (1) in fractal geometries. Even the simplified expression for spectrum (11) is quite difficult to analyze by itself, therefore, we need to introduce dynamical systems and study its action on an interval. We start with the spectrum of an elementary block, and each iteration of the corresponding dynamical system gives the spectrum of the next iteration of a fractal. The limit set of the dynamical system (i.e., the limit of an infinite number of iterations) is equal to the spectrum of infinite iterations of a fractal.

Although it is not possible to represent Eq. (11) as a dynamical system without additional normalization, nevertheless, our approach is simple and does not influence the properties of the spectrum. Non-normalized eigenvalues x_{k+1} of the $(k + 1)$th iteration are obtained from eigenvalues of the kth iteration by an action of functions F_i,

$$x_{k+1} = F_i(x_k) = 1 + \epsilon \lambda_i x_k. \tag{12}$$

The resulting spectrum can be obtained via formula $\sigma(\hat{A}_k) = \{\lambda_i x_k\}$ with $x_0 = 1$. Another way to express the spectrum $\sigma(\hat{A}_k)$ is to consider all $k + 1$ iterations of Eq. (12) in the following:

$$\sigma(\hat{A}_k) = \left\{ \frac{\left(F_{i_{k+1}} \circ F_{i_k} \circ \cdots \circ F_{i_1}\right)(1) - 1}{\epsilon} \right\}. \tag{13}$$

Equation (13) shows that the spectrum is obtained from the limit set of translation and rescaling. Statistical properties of the spectrum are independent of them, and in order to study spectral properties, we can consider just the dynamical system without the last step of translation and rescaling.

One can regard the spectrum as the splitting process of eigenvalues on each iteration with a weight factor ϵ. The splitting can be represented as a tree, starting from the eigenvalues of the matrix a of the building block, and, in each iteration, every eigenvalue splits to points with a number equal to the rank of the matrix a. Despite simplicity of the process, this model already demonstrates a nontrivial structure of the spectrum.

The level-spacing distribution can be calculated straightforwardly when there is no intersection between branches in the tree. This condition depends also on properties of eigenvalues. If all eigenvalues of the matrix a are positive, the condition of the absence of intersection between branches is as follows:

$$\min |\lambda_i - \lambda_{i+1}| < \frac{1}{1 - \epsilon \lambda_{\max}} - \frac{1}{1 - \epsilon \lambda_{\min}}. \tag{14}$$

If there is no intersection between branches, the level-spacing distribution $P(s)$ follows a power-law distribution and becomes ∞ when $s = 0$. Precisely, $P(s)$ is a bunch of δ functions with a power-law envelope [see Fig. 1(a) as an example].

For the cases when the number of intersections is small, if we increase the weighting factor ϵ, these δ functions begin to smear and drift closer to each other, and the slope of the level-spacing distribution $P(s)$ increases [an example of smeared δ
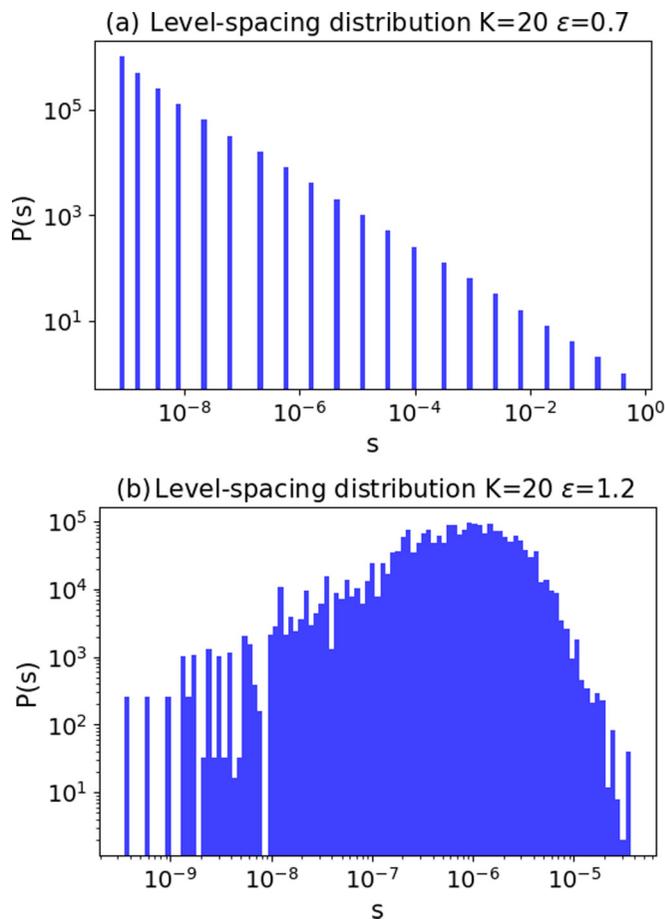

FIG. 1. Level-spacing distribution $P(s)$ for a simple model of the dynamical system with two eigenvalues $\{-1/2, 1/2\}$ after 20 iterations, exact power-law, and after the transition point. $\epsilon = 0.7$ in (a) and $\epsilon = 1.2$ in (b).

functions can be seen from the statistics of a real fractal in Fig. 3(a)]. Then, at some critical point, when the smeared δ functions are close enough to each other, there is a transition to another profile without the obvious power-law envelope. This profile qualitatively follows the level-spacing statistics of disordered systems. For example, $P(s)$ goes to zero for smaller s and has fast decay for larger s [see Fig. 1(b)].

In order to show that kind of transition more clearly, let us consider first the simple model with two eigenvalues $\{-1/2, 1/2\}$. If $\epsilon < 1$, one can obtain a power-law level-spacing distribution [see Fig. 1(a)],

$$P(s) \sim \left(\frac{s}{1 - \epsilon} \right)^{\ln 2/(\ln \epsilon - \ln 2)}. \tag{15}$$

At the critical point $\epsilon = 1$, the limit set is continuous in the interval $[-1, 1]$. At each iteration, all eigenvalues are equidistant from the neighboring eigenvalues, and, therefore, a power-law distribution becomes a δ function, which drifts to zero with increasing the number of iterations.

If $\epsilon > 1$, there is no singularity in $P(s)$ at $s = 0$, because of the mixing of tree branches [see an example shown in Fig. 1(b)]. The exact power-law symmetry of consequent splitting is broken.
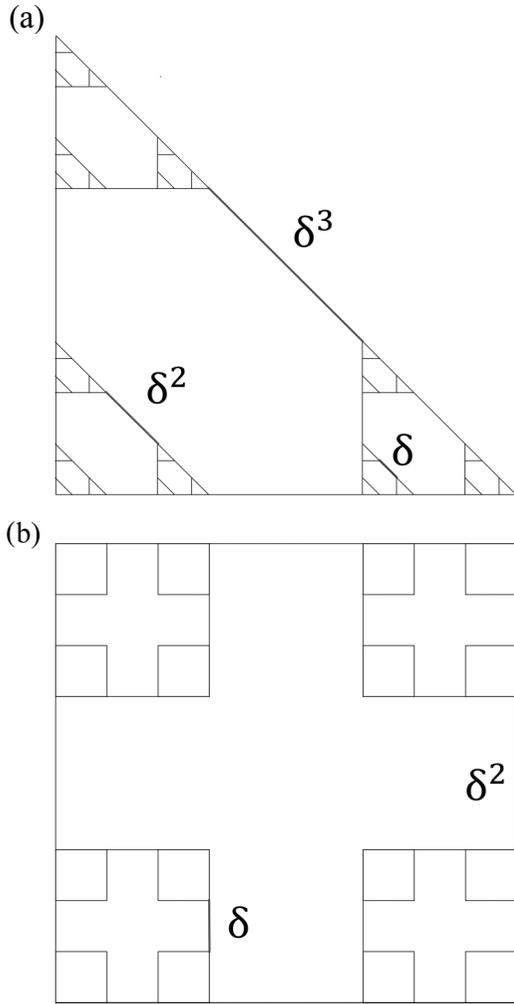
(a)

(b)

FIG. 2. Three iterations of the extended Sierpinski carpet and two iterations of the extended square. The blue edges correspond to the neighboring weight. All edges of the same scale have the same weight.
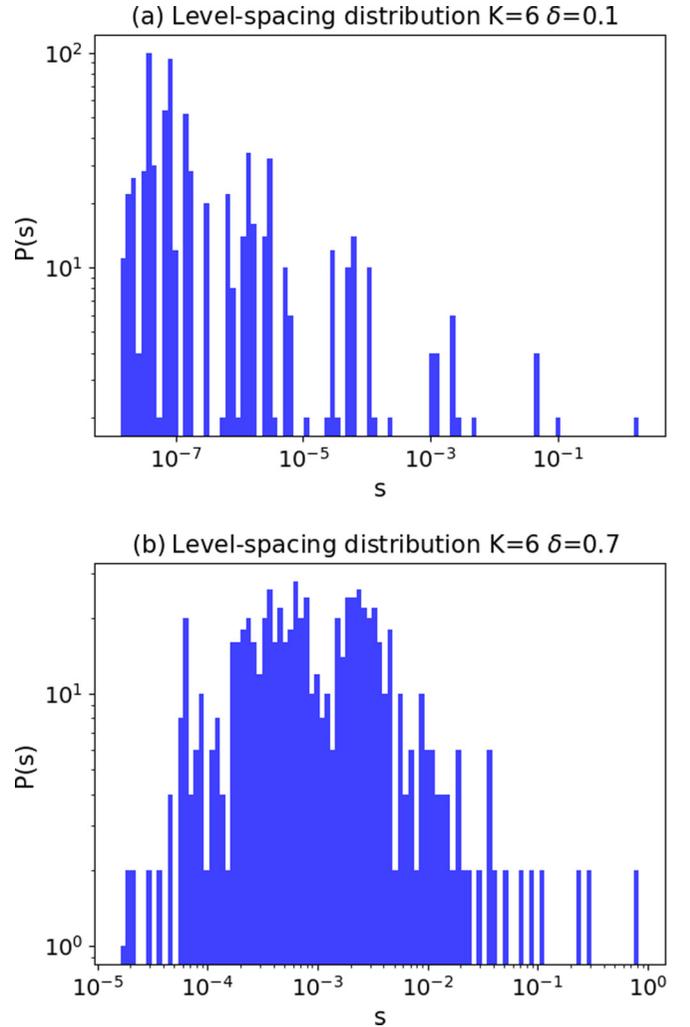

FIG. 3. Level-spacing distribution of six iterations of the hierarchical graph with the square blocks, $\delta = 0.1$ and $\delta = 0.7$. The top demonstrates power-law behavior, and the bottom one does not have obvious power-law dependence.

Despite the simplicity of the above model, the features of general nonlinear iterations of functions will be captured correctly for the following reasons. If we consider the invariant interval of a dynamical system, then, there are two possibilities, namely, the invariant interval either contains a gap or not. If there is a gap, then, after one iteration, this gap will be mapped into another one with smaller size and so on. The limit set is a Kantor set, and, in many cases, it has a power-law level-spacing distribution [36]. This case corresponds to the nonintersection of branches in a linearized version. If there is no gap, then, the distribution of points after one iteration becomes effectively more chaotic, which corresponds to intersection of different branches. Thus, we can distinguish three types of dynamical systems: fractal (without branches intersection), qualitatively chaotic (with intersections), and the one corresponding to the transition point between these two. One can speculate that a system with a smooth profile of density of states corresponds exactly to the transition point between intersection and nonintersection regimes.

IV. EXAMPLES

As was mentioned before, our approximation, such as presented in Eq. (11), works better if there are less connections between blocks. One of the best examples is to use cycles with one connection edge for a neighbor and add scaling parameter δ between blocks, such as our previous studies in Ref. [36] using the extended Sierpinski gasket shown in Fig. 2, here, one cycle consists of three vertices, therefore, $\epsilon = \delta/3$. Another example of a fractal that we studied is the extended square with one connection between two blocks, therefore, $\epsilon = \delta/4$.

For a fractal of the extended square, the building block is a square with four sites described by Hamiltonian Eq. (1) with $t = 1$. The eigenvalues of this building block are $\{-2, 0, 2\}$, therefore, the dynamical system is very similar to the simplest case considered in the previous section. The transition point is equal to $\epsilon = 0.25$, which corresponds to $\delta = 1$ with the critical exponent $2 \ln 2/\ln(2/9)$ (which is $\simeq -0.92$). This is the case without additional weighting on the edges. The critical point in the case of the extended Sierpinski gasket
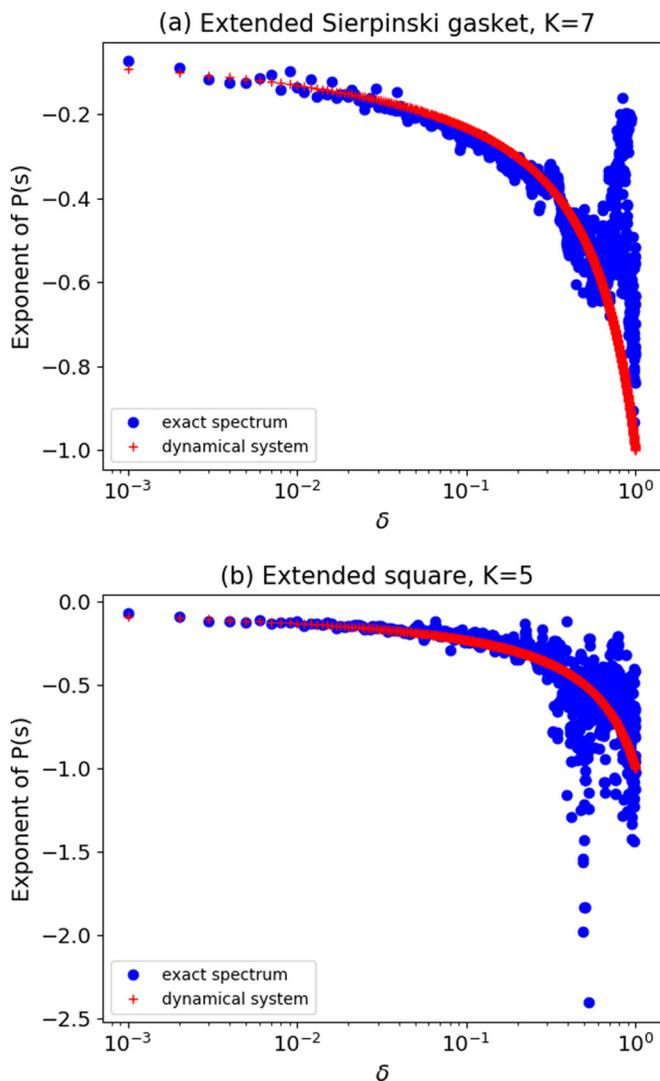
FIG. 4. Dependence of the exponent of the power-law distribution as a function of δ for the extended Sierpinski gasket (with seven iterations) and the extended square (with five iterations). The blue dots are obtained by exact diagonalization, and the red crosses are obtained by our approaches with the dynamical system.

is $\epsilon = 1/3$, which also corresponds to $\delta = 1$. This can be shown by an analysis of the invariant interval of the dynamical system.

We can see a power-law distribution with smeared peaks for the extended Sierpinski gasket in Fig. 3(a) on the contrary to Fig. 3(b), there is no power-law dependence. If there are no intersections in the splitting tree, the power-law spectrum is exact even with a finite number of iterations. However, if there are intersections, δ functions in $P(s)$ are smeared (as in the case of the exact spectrum), therefore, if s is close to 0, the level-spacing distribution function $P(s)$ will be determined by tails of smeared δ functions. Thus, a power-law dependence appears only in some range, even before δ approaches the transition point.

The above explanation is verified by our numerical calculations. In Fig. 4, the exponents of the power-law level-spacing distribution of fractals and their corresponding dynamical

systems are shown. We used seven iterations of the extended Sierpinski gasket, five iterations of the extended square, and the same number of iterations for the dynamical systems. We calculated the exponent of the power law for different δ's using linear regression on the log-scale before the level-spacing distribution reaches the maximum, i.e., we performed a cutoff on small δ. The dots of the exact spectrum for small δ demonstrate clear power-law behavior, and we see that with increased values of δ there are large fluctuations in the exponents.

If we compare the results obtained from the dynamical system to the exact spectrum, they match well for small values of δ, in some cases even for $\delta > 0.1$. In Fig. 5, we show more results for different iterations of extended Sierpinski gasket and the corresponding dynamical systems. One can see that, with increasing the number of iterations, the agreement between the two approaches is also better. Therefore, we conclude that, despite the fact that there should be an exact power law for an infinite fractal, and if we consider only finite iterations, this power law is not evident.

Large fluctuations in the exact spectrum when δ approaches its critical value can be understood in the following way. Around the critical point, the effective splitting converges very slowly with the number of iterations, so the number of iterations has to be very large. This issue is demonstrated in Fig. 5 in which we compare numerical results for various iterations of the dynamical system described by Eq. (15) and their theoretical predictions. We see that the numerical result with finite iterations always gives larger exponents than the theoretical prediction in the vicinity of the critical point. However, the accuracy of the numerical calculation increases with a larger number of iterations.

V. DIMENSION PROPERTIES

In this section, we study dimension properties of a graph, its spectrum, and their connections to level-spacing statistics. We also partially explain the results obtained in Ref. [7] where the authors found a connection between the dimension of the conductivity spectrum and the geometry dimension of the Sierpinski fractals.

In this section, we use the notion of Hausdorff dimension d_H. This dimension is a generalization of a topological dimension for nonregular geometric sets, such as fractals. The full mathematical definition is rather complicated, however, in many cases, the Hausdorff dimension admits a simple description. Suppose that $N(\epsilon)$ is the number of boxes of side length ϵ required to cover the set. Then, the Hausdorff dimension can be calculated as

$$d_H = \lim_{\epsilon \to 0} \frac{\ln N(\epsilon)}{\ln(1/\epsilon)}. \tag{16}$$

Roughly speaking, the dimension is the exponent relating the volume of a set with its characteristic linear size $V \sim L^{d_H}$, which is what one would expect in the case of a smooth space.

A. Sample and spectrum

First, let us discuss briefly the Hausdorff dimension of the spectrum. For a power-law spectrum, there are obviously gaps on all possible scales, therefore, the Hausdorff dimension
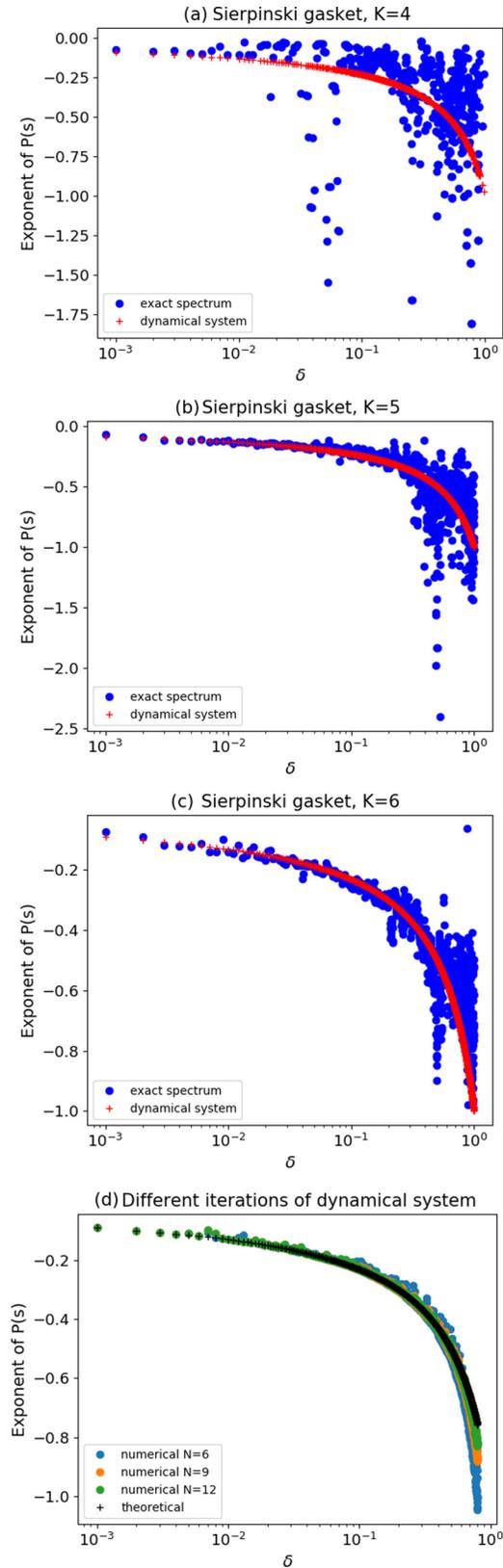
FIG. 5. (a)–(c) The comparison between the exact spectrum and the results obtained for the dynamical system with different iterations in the extended Sierpinski gasket. (d) The comparison between numerical and theoretical results for the dynamical system.

cannot be equal to one. Actually, one can extend the idea of gaps at all scales as a criterion of fractional dimension. However, there is a subtlety in the limit procedure.

Let us consider the same toy model with two eigenvalues $\{-1/2, 1/2\}$ as the one we have studied. We have seen that there are two regimes with different properties depending on the value of ϵ: $\epsilon < 1$ and $\epsilon > 1$. The spectrum for $\epsilon < 1$ is the Cantor set, and its Hausdorff dimension is $d_s = -\ln 2/(\ln \epsilon - \ln 2)$. One may note that the Hausdorff dimension of the spectrum corresponds to the exponent in the power law of the level-spacing distribution shown in Eq. (15), i.e., $P(s) \sim s^{-d_s}$. One can assume that the same result should hold for the multiscale Cantor set (the Cantor set, which is obtained by deleting intervals of various fractions), which also corresponds to the approximation for a general spectral decimation function [36]. We want to remind that the Hausdorff dimension discussed here is not the spectral dimension of the density of states.

The Hausdorff dimension of the spectrum of the above simple model can be obtained from the relation $d_s = \ln(2)/\ln[(1 - \Delta_1/\Delta)/2]$, where $\Delta = 1/(1 - \epsilon/2)$ is the energy range of the spectrum (or invariant set of the dynamical system), and $\Delta_1 = (1 - \epsilon)/(1 - \epsilon/2)$ is the largest gap in the limit set of the dynamical system. This formula can be understood in the following way. Since our dynamical system is linear, after the second iteration, the biggest gap Δ_1 repeats itself on the lower scale with some constant scaling factor. These new gaps repeat again with the same scaling factor and so on. Thus, we can deduce the Hausdorff dimension from the first gap alone.

If $\epsilon = 1$ as was discussed before, in the limit set, when the number of iterations approaches infinity, the values spread completely over $[-1, 1]$, and, therefore, the Hausdorff dimension is 1. If $\epsilon > 1$, gaps become smaller and smaller after each iteration (one can see this from Fig. 1), the limit set does not contain any gaps, and its Hausdorff dimension is also 1.

The estimation of the Hausdorff dimension of a hierarchical graph is more difficult since the correct value is related to the embedding of a graph into a plane. However, it is possible for fractals with building blocks, which can tessellate an n-dimensional space, i.e., for a two-dimensional (2D) plane they are the triangle, square, and honeycomb lattices. Furthermore, there could be another problem occurring, if one takes a number of connections between blocks into account. Nevertheless, we can estimate the Hausdorff dimension by the following procedure. Basically, the concept behind the dimension is how many new copies appear when we increase the length of a sample $N_{new} \sim l^{d_G}$, where d_G is the dimension of the sample. Therefore, one key issue is an estimation of a proper choice of the length change. If there is an embedding into a space with integer dimension, it can be obvious. In general, we need to work only with the number of vertices n_v and the number of connections n_c. The number of connections is related to the effective length, and the number of vertices determines the number of new copies N_{new}. Hence, we can estimate the dimension of a graph Γ as $d_\Gamma \sim \ln n_v/\ln 2n_c$. For the Sierpinski gasket, we have $n_v = 3$ and $n_c = 1$, and we obtain $d_\Gamma \sim \ln 3/\ln 2$, which is the correct result.

For hierarchically weighted graphs, one can consider an additional weighting δ as in the previous section and obtain

an effective dimension $d_\Gamma \sim \ln n_v / \ln(2n_c/\delta)$. Furthermore, one can relate the dimension of the spectrum in the previous section and the estimated dimension of a weighted fractal square. For this system, we have $n_v = 4$ and $n_c = 1$, and we obtain $d_s = \ln 2/(\ln 2 - \ln \delta)$ and $d_\Gamma \sim 2 \ln 2/(\ln 2 - \ln \delta)$. d_s and d_Γ are not the same, but they differ only with a multiplier constant. However, we see that there is a deep relation between the dimension of the spectrum and the dimension of a fractal. For example, we can note that, if $\delta \to 0$, then, both dimensions d_Γ and d_s go to zero. Therefore, we can conclude that a system with a small Hausdorff dimension should have a power-law level-spacing distribution.

B. Conductance

The conductance of a fractal can be calculated via the Landauer formula [38],

$$G(E)_{ll'} = \frac{e^2}{h} \operatorname{Tr} \left(\Gamma_l G_S^r \Gamma_{l'} G_S^a \right), \tag{17}$$

where l and l' are indices of leads, G_S^r and G_S^a are retarded, and advanced Green's functions, Γ_l and $\Gamma_{l'}$ take into account corrections to the self-energy regarding the interaction with leads. The Green's functions have poles at points in the spectrum.

Dimension of the graph of $G(E)$ is related to the dimension of the spectrum of a sample. If there is no correlation between eigenstates, the dimension of $G(E)$ equals to the dimension of discontinuity points in dG/dE (which is equal to the dimension of the spectrum) plus one. The correlations between eigenstates will smooth the discontinuity.

Therefore, we arrive at

$$d_H(G) \leqslant 1 + d_s. \tag{18}$$

In our approach based on the introduction of the auxiliary dynamical system, all eigenvectors are just tensor products of eigenvectors of a building block. Thus, all scalar products of eigenfunctions and matrices of leads (Γ_l, Γ_l') can be calculated, and the conductivity will have nonregular fractal structure on all scales. At every pole of the Green's functions, there is a discontinuity, and Eq. (18) becomes an equality within the considered approximation. As we discussed in the previous section, if a sample has a power-law distribution of $P(s)$, its geometry dimension can be expressed as the dimension of spectrum with some multiplier (see the case of the weighted fractal square). This multiplier depends on the structure of the building block (its' eigenvalues), and, therefore, there is no universal formula between $d_H(G)$ and d_Γ.

A subtle case appears at the transition point when d_s is close to 1. In this case, the inequality expressed in Eq. (18) is trivial, and the dimension of the spectrum provides no information about the conductance. Effectively, the spectrum is dense, and the Green's functions have singularities on a continuous interval. The studied Sierpinski carpet in Ref. [7] seems to be this case.

VI. SUMMARY AND DISCUSSION

In this paper, we consider the linearized version of spectral decimation within an approach based on the dynamical system for hierarchical graphs with block structures. We demonstrate that the power-law level-spacing statistics appearing in some fractals is closely related to their geometry. Our approach to calculate the level-spacing distribution shows different behaviors depending on the fractal structure. It was shown that the level-spacing distribution can have strictly a power-law behavior or resemble behavior of a quantum chaotic system.

The power-law spectrum is closely connected to the ramification number of a fractal, however, the actual distinction is quite subtle. There could be infinitely ramified fractals with power-law spectra as well as finitely ramified with spectra closer to disordered systems. We suppose that a variation of the Sierpinski carpet with two vertices between connected elementary blocks instead of three has a power-law level-spacing distribution. An opposite example of a finitely ramified fractal with disordered spectrum statistics can be realized if the number of vertices in an elementary block is large enough, and its eigenvalues are close to each other so that there will be no gaps in the limit set of the dynamical system generating the spectrum. The correct analysis of possible statistical properties should require an individual consideration in each case since it depends on the eigenvalues of the building block of a hierarchical structure.

Our approach based on the theory of dynamical systems can also explain the results concerning recently discovered topological effects in fractals. It is also well known that there is a quantum Hall effect in 2D but not in one dimension (1D). In Refs. [16,39,40], it was shown that Chern numbers as well as Hall conductivity become partially quantized in noninteger dimensions. In view of the present paper, the actual transition from quantized topological properties in 2D to their destruction in 1D could be followed from the change in hierarchical block structure of a graph and the corresponding dynamical system on its spectrum. Since our model can be treated analytically, one can calculate Chern numbers and topological states, for example, using expression for the Chern number via projectors. One can expect different behaviors of projectors depending on the regime of linearized spectral decimation. Our future research will be devoted to these questions.

To summarize, from the perspective of considered estimation, we can treat random graphs as deformations of the graphs with a block hierarchical structure. The additions of various building blocks and variations of connections between them lead to mixing of splitting branches, and, therefore, the power-law statistics disappears, and the system becomes closer to a disordered system. Our paper can lead to a clearer distinction between quantum chaotic systems, systems with fractal geometries and quasiperiodic systems. As was mentioned earlier, our paper can also be useful for investigations of topological properties, such as topological states and Chern numbers.

APPENDIX: GEOMETRIC INTERPRETATION OF THE MODEL

The density of states of the Hamiltonian can be calculated via traces of the Hamiltonian in some power, which can be expressed by the number of connected paths in a graph corresponding to the Hamiltonian. In the case of the Cartesian product of graphs, one can estimate the trace of a matrix power as

$$\mathrm{tr}(H \square G)^m = p_m(H \square G) \sim \sum_{l=0}^{m} C_m^l p_{m-l}(G) p_l(H), \quad (A1)$$

where p_n is the number of loops and index n is the number of sites in this loop (length of the loop). This expression is exact, if each point in graphs A or H is indistinguishable. The full expression of p_m is as follows:

$$p_m(H \square G) = \sum_{x \in A, H} \sum_{l=0}^{m} C_m^l p_{m-l}(G_x) p_l(H_x). \quad (A2)$$

The block structure of a fractal graph can be represented by tensor product, which is closely related to the Cartesian product. The expressions (9) and (10) have tensor structures. From the geometric point of view, these formulas can be derived in the following. A point p_0 in $H \square G$ can be projected into H or G, so p_0 has two coordinates. If we want to create a path between p_0 and another point p_1, we can project this path onto coordinates in H or in G. By the structure of a Cartesian product, we can always choose coordinates in H or in G, and can combine closed paths and obtain Eq. (A2).

Let us consider the case when the number of connections between two neighboring copies of graph H is less than the number of vertices (i.e., the number of connections in the Cartesian product). Let us denote this matrix as $H * G$. In this case, a point p_0 also has two coordinates, however, we cannot change make a new step in each of the projections at arbitrary points. But we can make an estimation, saying that the number of closed paths in G coordinate will be proportional to the number of paths in Eq. (A2). With this approximation, we neglect details of the geometry and use only the number of connections between blocks. The coefficient of proportionality ϵ will be equal to fraction n_c/n_v, where n_c is the number of connections and n_v is the number of vertices in a graph H,

$$\mathrm{tr}(H * G)^m = p_m(H * G) \sim p_m(H) p_0(G)$$
$$+ \sum_{l=0}^{m-1} \epsilon^{m-l} C_m^l p_{m-l}(G) p_l(H). \quad (A3)$$

If a graph G can be embedded into a graph E, it is an obvious relation that $p_n(G) \leqslant p_n(E)$. Because of the block structure, a fractal can be embedded (at least, locally) into the Cartesian product, and we can apply this inequality. For fractals, roughly, connections between blocks on different scales are described by matrix $A_0 = a$. If we directly apply expression (A3), it will correspond to $c \sim 1$ in Eq. (10). Although this is also an estimation, but it does not include mixing of different scales on the density of states [mixing of scales appears when one tries to estimate traces from Eq. (6) due to noncommutativity]. The model with $c \sim 1$ describes splitting of eigenvalues with the same order every time.

In order to add an influence of each scale to another, we can say that, when we construct a path, every step on a larger scale is also a step in smaller scales but with some weight ϵ. Then, the trace of A_2^m,

$$\mathrm{tr}\left(A_2^m\right) \sim p_m(a) n_v^m + \sum_{l=0}^{m-1} \epsilon^{m-l} C_m^l p_{m-l}(a) p_m(a). \quad (A4)$$

The formulas for greater iterations of the fractal are cumbersome, but from the main text, it is already clear this case corresponds to Eqs. (10) and (11) with $c \sim a$.

We can formulate the model of this article as follows. We build an effective model for the density of states of a fractal assuming that we only know the number of connections from one block to other.

Of course, there can be other effective models with various weights on different scales. However, the model considered in this article clearly exploits the scale symmetry of a system. If the detailed geometry does not have strict scale symmetry (for example, connections between blocks are in different places in every scale), then, appropriate weighting of paths could be different, or the nonlinearity could play a stronger role.

[1] M. Polini, F. Guinea, M. Lewenstein, H. C. Manoharan, and V. Pellegrini, Artificial honeycomb lattices for electrons, atoms and photons, Nat. Nanotechnol. **8**, 625 (2013).

[2] M. Gibertini, A. Singha, V. Pellegrini, M. Polini, G. Vignale, A. Pinczuk, L. N. Pfeiffer, and K. W. West, Engineering artificial graphene in a two-dimensional electron gas, Phys. Rev. B **79**, 241406(R) (2009).

[3] J. Shang, Y. Wang, M. Chen, J. Dai, X. Zhou, J. Kuttner, G. Hilt, X. Shao, J. M. Gottfried, and K. Wu, Assembling molecular Sierpinski triangle fractals, Nat. Chem. **7**, 389 (2015).

[4] S. N. Kempkes, M. R. Slot, S. E. Freeney, S. J. M. Zevenhuizen, D. Vanmaekelbergh, I. Swart, and C. Morais Smith, Design and characterization of electrons in a fractal geometry, Nat. Phys. **15**, 127 (2018).

[5] X.-Y. Xu, X.-W. Wang, D.-Y. Chen, C. Morais Smith, and X.-M. Jin, Shining light on quantum transport in fractal networks, arXiv:2005.13385.

[6] Z. Yang, E. Lustig, Y. Lumer, and M. Segev, Photonic Floquet topological insulators in a fractal lattice, Light: Sci. Appl. **9**, 128 (2020).

[7] E. van Veen, S. Yuan, M. I. Katsnelson, M. Polini, and A. Tomadin, Quantum transport in Sierpinski carpets, Phys. Rev. B **93**, 115428 (2016).

[8] E. van Veen, A. Tomadin, M. Polini, M. I. Katsnelson, and S. Yuan, Optical conductivity of a quantum electron gas in a Sierpinski carpet, Phys. Rev. B **96**, 235438 (2017).

[9] Z.-G. Song, Y.-Y. Zhang, and S.-S. Li, The topological insulator in a fractal space, Appl. Phys. Lett. **104**, 233106 (2014).

[10] T. Westerhout, E. van Veen, M. I. Katsnelson, and S. Yuan, Plasmon confinement in fractal quantum systems, Phys. Rev. B **97**, 205434 (2018).

[11] T. G. Pedersen, Graphene fractals: Energy gap and spin polarization, Phys. Rev. B **101**, 235427 (2020).

[12] D. Sticlet and A. Akhmerov, Attractive critical point from weak antilocalization on fractals, Phys. Rev. B **94**, 161115(R) (2016).

[13] A. Kosior and K. Sacha, Localization in random fractal lattices, Phys. Rev. B **95**, 104206 (2017).

[14] B. Pal and A. Chakrabarti, Staggered and extreme localization of electron states in fractal space, Phys. Rev. B **85**, 214203 (2012).

[15] B. Pal, P. Patra, J. P. Saha, and A. Chakrabarti, Engineering wave localization in a fractal waveguide network, Phys. Rev. A **87**, 023814 (2013).

[16] M. Brzezinska, A. M. Cook, and T. Neupert, Topology in the Sierpinski-Hofstadter problem, Phys. Rev. B, **98**, 205116 (2018).

[17] A. Agarwala, S. Pai, and V. B. Shenoy, Fractalized metals, arXiv:1803.01404.

[18] S. Manna, B. Pal, W. Wang, and A. E. B. Nielsen, Anyons and fractional quantum Hall effect in fractal dimensions Phys. Rev. Res. **2**, 023401 (2020).

[19] S. Pai and A. Prem, Topological states on fractal lattices, Phys. Rev. B **100**, 155135 (2019).

[20] G. Bouzerar and D. Mayou, Quantum transport in self-similar graphene carpets, Phys. Rev. Res. **2**, 033063 (2020).

[21] B. Pal and K. Saha, Flat bands in fractal-like geometry, Phys. Rev. B **97**, 195101 (2018).

[22] A. Nandy, B. Pal, and A. Chakrabarti, Flat band analogues and flux driven extended electronic states in a class of geometrically frustrated fractal networks, J. Phys.: Condens. Matter **27**, 125501 (2015).

[23] A. Nandy and A. Chakrabarti, Engineering slow light and mode crossover in a fractal-kagome waveguide network, Phys. Rev. A **93**, 013807 (2016).

[24] A. Nandy, Controlled quantum imprisonment of wave packet and flat bands in a fractal geometry, arXiv:2005.03688.

[25] A. K. Golmankhaneh, Statistical mechanics involving fractal temperature, Fractal Fract. **3**, 20 (2019).

[26] A. K. Golmankhaneh and C. Tunc, Analogues to lie method and noether's theorem in fractal calculus, Fractal Fract. **3**, 25 (2019).

[27] M. S. Vasconcelos and M. G. Cottam, Plasmon-polariton fractal spectra in quasiperiodic photonic crystals with graphene, Europhys. Lett. **128**, 27003 (2019).

[28] I. Akal, Entanglement entropy on finitely ramified graphs, Phys. Rev. D **98**, 106003 (2018).

[29] T. Shima, On eigenvalue problems for laplacians on P. C. F. self-similar sets, Japan J. Indust. Appl. Math. **13**, 1 (1996).

[30] E. Domany, S. Alexander, D. Bensimon, and L. Kadanoff, Solutions to the Schrödinger equation on some fractal lattices, Phys. Rev. B **28**, 3110 (1983).

[31] W. Schwalm and B. Moritz, Continuous spectra of a family of lattices containing the modified rectangle lattice of Dhar, Phys. Rev. B **71**, 134207 (2005).

[32] D. Dhar, Lattices of effectively nonintegral dimensionality, J. Math. Phys **18**, 577 (1977).

[33] D. Dhar, Self-avoiding random walks: Some exactly soluble cases, J. Math. Phys **19**, 5 (1978).

[34] K. Machida and M. Fujita, Quantum energy spectra and one-dimensional quasiperiodic systems, Phys. Rev. B **34**, 7367 (1986).

[35] M. Naka, K. Ino, and M. Kohmoto, Critical level statistics of the Fibonacci model, Phys. Rev. B **71**, 245120 (2005).

[36] A. Iliasov, M. I. Katsnelson, and S. Yuan, Power-law energy level spacing distributions in fractals, Phys. Rev. B **99**, 075402 (2019).

[37] J. C. Collins, *Renormalization* (Cambridge University Press, Cambridge, UK, 1984).

[38] S. Datta, *Electronic Transport in Mesoscopic Systems* (Cambridge University Press, Cambridge, UK, 1997).

[39] A. Iliasov, M. I. Katsnelson, and S. Yuan, Hall conductivity of a Sierpiński carpet, Phys. Rev. B **101**, 045413 (2020).

[40] M. Fremling, M. van Hooft, C. Smith, and L. Fritz, Existence of robust edge currents in Sierpiński fractals, Phys. Rev. Res. **2**, 013044 (2020).